axioms

MDPI

Article

New Two-Level Time-Mesh Difference Scheme for the Symmetric Regularized Long Wave Equation

Jingying Gao *, Qingmei Bai, Siriguleng He and Eerdun Buhe

School of Mathematics Science, Hohhot Minzu College, Hohhot 010051, China;
baiqingmei@email.imnc.edu.cn (Q.B.); t53000839@email.imnc.edu.cn (S.H.); eerdunbuhe@163.com (E.B.)
* Correspondence: minzugjy@email.imnc.edu.cn

Abstract: The paper introduces a new two-level time-mesh difference scheme for solving the symmetric regularized long wave equation. The scheme consists of three steps. A coarse time-mesh and a fine time-mesh are defined, and the equation is solved using an existing nonlinear scheme on the coarse time-mesh. Lagrange's linear interpolation formula is employed to obtain all preliminary solutions on the fine time-mesh. Based on the preliminary solutions, Taylor's formula is utilized to construct a linear system for the equation on the fine time-mesh. The convergence and stability of the scheme is analyzed, providing the convergence rates of $O(\tau_F^2 + \tau_C^4 + h^4)$ in the discrete L_∞-norm for $u(x,t)$ and in the discrete L_2-norm for $\rho(x,t)$. Numerical simulation results show that the proposed scheme achieves equivalent error levels and convergence rates to the nonlinear scheme, while also reducing CPU time by over half, which indicates that the new method is more efficient. Furthermore, compared to the earlier time two-mesh method developed by the authors, the proposed scheme significantly reduces the error between the numerical and exact solutions, which means that the proposed scheme is more accurate. Additionally, the effectiveness of the new scheme is discussed in terms of the corresponding conservation laws and long-time simulations.

Keywords: SRLW equation; finite difference; second-order; two-level time-mesh; convergence analysis

MSC: 65M06

Citation: Gao, J.; Bai, Q.; He, S.; Buhe, E. New Two-Level Time-Mesh Difference Scheme for the Symmetric Regularized Long Wave Equation. *Axioms* **2023**, *12*, 1057. https://doi.org/10.3390/axioms12111057

Academic Editors: Behzad Djafari-Rouhani and Luis Vázquez

Received: 13 October 2023
Revised: 12 November 2023
Accepted: 14 November 2023
Published: 17 November 2023

1. Introduction

In this paper, the following initial boundary value problem of the symmetric regularized long wave (SRLW) Equation [1] is considered:

$$\begin{cases} u_t + \rho_x + uu_x - u_{xxt} = 0, \quad x_L \le x \le x_R, \ 0 < t \le T, \\ \rho_t + u_x = 0, \quad x_L \le x \le x_R, \ 0 < t \le T, \\ u(x_L,t) = u(x_R,t) = 0, \quad \rho(x_L,t) = \rho(x_R,t) = 0, \quad 0 < t \le T, \\ u(x,0) = u_0(x), \quad \rho(x,0) = \rho_0(x), \quad x_L \le x \le x_R, \end{cases} \tag{1}$$

where $u(x,t)$ and $\rho(x,t)$ are the fluid velocity and the density, respectively.

The SRLW equation is a partial differential equation that takes into account the effects of dispersion and nonlinearity utilized to depict a range of physical phenomena such as nonlinear optics, fluid dynamics, and quantum mechanics. In nonlinear optics, it is employed to study the propagation of optical pulses in materials with nonlinear properties. In fluid dynamics, it is used to model the behavior of shallow water waves and to study wave interactions in coastal regions. In quantum mechanics, it is applied to describe the dynamics of Bose–Einstein condensates and other quantum systems. Currently, many researchers have employed various methods to obtain exact traveling and solitary wave solutions for the SRLW equation, such as the exp-function method [2], (G'/G)-expansion method [3], Lie symmetry approach [4], analytical method [5], sine–cosine method [6], etc.

Significant achievements have also been made in the research of numerical solutions for the SRLW equation. Guo [7] conducted a study on the existence, uniqueness, and regularity of numerical solutions for the periodic initial value problem of the generalized SRLW equation using the spectral method. Zheng et al. [8] proposed a Fourier pseudospectral method with a restraint operator for the SRLW equation that demonstrated stability and optimal error estimates. Shang et al. [9] analyzed a Chebyshev pseudospectral scheme for multi-dimensional generalized SRLW equations. Fang et al. [10] studied the presence of global attractors of the SRLW equation. Wang et al. [11] investigated a coupled two-level and nonlinear-implicit finite difference method for solving the SRLW equation, achieving second-order accuracy in both space and time. Bai et al. [12] studied a finite difference scheme with two layers for the SRLW equation, which is a conservative scheme and converges with an order of $O(\tau + h^2)$ in the L^∞ norm for u and in the L_2 norm for ρ. Xu et al. [13] solved a dissipative SRLW equation containing a damping term using a mixed finite element method. Yimnet et al. [14] introduced a novel finite difference method in which a new average difference technique with four levels is employed to solve the u independently from the ρ of the SRLW equation. In order to achieve better solving results, many researchers have constructed difference schemes with higher convergence orders. Nie [15] constructed a decoupled finite difference scheme with fourth-order accuracy for solving the SRLW equation. Hu et al. [16] introduced a novel conservative Crank–Nicolson finite difference scheme for the SRLW equation. This scheme achieves an accuracy of $O(\tau^2 + h^4)$ without refined mesh. Kerdboon et al. [17] proposed a three-point compact difference scheme for the SRLW equation. He et al. [18] presented a compact difference scheme with four time-levels for the SRLW equation. The scheme is constructed for the SRLW equation with a sole nonlinear velocity term and exhibits a high accuracy of $O(\tau^2 + h^4)$. However, most of the high convergence accuracy scheme deal with the points near the boundary via the use of ghost points or fictitious points. Li et al. [19] proposed a compact scheme for the SRLW equation that avoids the use of ghost points by utilizing inverse compact operators. He et al. [20] also proposed a novel conservative three-point linearized compact difference scheme to handle the challenges posed by discrete boundaries and nonlinear terms in solving SRLW equations.

The combination of the time two-mesh (TT-M) technique [21–27] with other numerical methods also can improve the efficiency of solving nonlinear partial differential equations. Liu et al. [21] investigated a finite element method with the TT-M technique, which was successfully applied to solve the fractional water wave model and other fractional models. Afterward, other authors [22–26] used the TT-M method to study the numerical solutions for the partial differential equations such as the Allen–Cahn model, Sobolev model and the nonlinear Schrödinger equation. Gao et al. [27] introduced a TT-M finite difference scheme for the SRLW equation, achieving first-order accuracy in time and second-order accuracy in space. However, the error in the numerical solutions of the scheme increases rapidly over a long time period, making it hard to simulate the long-time behavior of Equation (1).

To improve the efficiency and accuracy of numerical schemes for the SRLW equation, in this paper, we construct a second-order two-level time-mesh finite difference scheme based on the nonlinear scheme in [16]. As a result, the proposed scheme achieves a convergence rate of $O(\tau_F^2 + \tau_C^4 + h^4)$ in the discrete L_∞-norm for $u(x,t)$ and in the discrete L_2-norm for $\rho(x,t)$. The proposed scheme has several advantages: (i) Combined with the two level time-mesh technique, the scheme utilizes the nonlinear scheme on a coarse time-mesh and then constructs a linear difference system on a fine time-mesh, which more efficiently solves the SRLW equation than the nonlinear scheme in [16]; (ii) The new scheme obtains a high accuracy in solving the SRLW equation. The proposed scheme has a second-order convergence rate in time and a fourth-order convergence rate in space, which is higher than that of the scheme in [27]; (iii) The convergence and stability of the scheme have been verified through detailed proofs. Theoretical analysis of the scheme is more intricate compared to existing TT-M methods since a function with three variables is used in the process of the linear system construction.

The rest of this article is structured as follows: Section 2 introduces the notations and lemmas. Following that, Section 3 outlines the construction of the two-level time-mesh finite difference numerical scheme. In Section 4, we delve into the convergence and stability of the scheme. Next, Section 5 offers numerical results to test the theoretical findings, computational efficiency, and accuracy of the scheme. Finally, in Section 6, we conclude the paper.

2. Some Notations and Lemmas

For time and space intervals $(0, T]$ and $[x_L, x_R]$, let $t_n = n\tau, (n = 1, 2, \ldots, [T/\tau] = N)$ be the time-level and $x_j = x_L + jh, (j = 0, 1, 2, \ldots, \frac{x_R - x_L}{h} = J)$ be the space mesh point, where τ and h represent time and space step sizes.

Let $Z_h^0 = \{u^n = (u_j^n) \mid u_{-1}^n = u_0^n = u_J^n = u_{J+1}^n = 0, j = -1, 0, 1, \ldots, J, J+1\}$ be the space of mesh functions, where $j = -1$ and $J + 1$ are ghost points. The following notations will be used in this paper:

$$\left(u_j^n\right)_x = \frac{u_{j+1}^n - u_j^n}{h}, \quad \left(u_j^n\right)_{\bar{x}} = \frac{u_j^n - u_{j-1}^n}{h}, \quad \left(u_j^n\right)_{\hat{x}} = \frac{u_{j+1}^n - u_{j-1}^n}{2h},$$
$$\left(u_j^n\right)_{\ddot{x}} = \frac{u_{j+2}^n - u_{j-2}^n}{4h}, \quad \left(u_j^n\right)_t = \frac{u_j^{n+1} - u_j^n}{\tau}, \quad u_j^{n+\frac{1}{2}} = \frac{u_j^{n+1} + u_j^n}{2},$$

M is used to denote a general positive constant, which may have different values in different locations.

We define the discrete inner product and norms with respect to any pair of mesh functions $u^n, w^n \in Z_h^0$ as follows:

$$(u^n, w^n) = h \sum_{j=1}^{J-1} u_j^n w_j^n, \quad \|u^n\| = \sqrt{(u^n, u^n)}, \quad \|u^n\|_\infty = \max_{1 \le j \le J-1} |u_j^n|.$$

Lemma 1 (See [16]). *For a mesh function $u^n \in Z_h^0$, by Cauchy–Schwarz inequality, we have*

$$\|u_{\ddot{x}}^n\|^2 \leqslant \|u_{\hat{x}}^n\|^2 \leqslant \|u_x^n\|^2.$$

Lemma 2 (See [18]). *If $u^n, w^n \in Z_h^0$ are two mesh functions, we have*

$$(u_x^n, w^n) = -(u^n, w_{\bar{x}}^n) = -(u^n, w_x^n), \quad (u_{x\bar{x}}^n, w^n) = -(u_x^n, w_x^n), \quad (u_{\hat{x}}^n, w^n) = -(u^n, w_{\hat{x}}^n).$$

Furthermore,

$$(u_{x\bar{x}}^n, u^n) = -\|u_x^n\|^2, \quad \|u_{\hat{x}}^n\| \le \|u_x^n\| = \|u_{\bar{x}}^n\|.$$

Lemma 3 (See [26]). *Assume that a sequence of non-negative real numbers $\{a_j\}_{j=0}^{\infty}$ satisfying*

$$a_{n+1} \le \alpha + \beta \sum_{j=0}^{n} a_j \tau, \quad n \ge 0,$$

has the inequality $a_{n+1} \le (\alpha + \tau\beta a_0) e^{\beta(n+1)\tau}$, where $\alpha \ge 0, \beta$ and τ are positive constants.

Lemma 4 (See [28]). *For a mesh function $u^n \in Z_h^0$, there exists constants C_1 and C_2, such that*

$$\|u^n\|_\infty \le C_1 \|u^n\| + C_2 \|u_x^n\|.$$

3. Construction of Two-Level Time-Mesh Difference Scheme

This article is inspired by the approach presented in [16], which involves a nonlinear implementation and requires a significant amount of CPU time. To address the problem, this study constructed a numerical difference scheme by incorporating the two-level time-mesh technique for the SRLW equation.

Prior to introducing the proposed scheme, we define the coarse time-mesh and the fine time-mesh. First, the time interval $(0, T]$ is equally divided into P small time intervals. This divided time-mesh is called a coarse time-mesh. Secondly, each small time interval is further partitioned into $s(2 \leq s \in Z^+)$ intervals. The mesh after this second segmentation is called a fine time-mesh. The coarse time-mesh has the time levels $t_{ks} = k\tau_C(k = 0, 1, \ldots, P)$ and $0 = t_0 < t_s < t_{2s} < \ldots < t_{Ps} = T$, and the fine time-mesh has the time levels $t_n = n\tau_F(n = 0, 1, 2, \ldots, Ps = N)$ and $0 = t_0 < t_1 < t_2 < \ldots < t_N = T$, where $\tau_C = s\tau_F$ and τ_F are the coarse and fine time step size, respectively. The combination of above two different time-meshes is referred to as a two-level time-mesh.

The two-level time-mesh difference scheme for the SRLW equation is presented as follows. Let $u_{C,j}^{ks} = u(x_j, t_{ks}), \rho_{C,j}^{ks} = \rho(x_j, t_{ks})$ be the numerical solutions on the coarse time-mesh, then we calculate the $u_{C,j}^{ks}$ and $\rho_{C,j}^{ks}$ by the following nonlinear scheme in [16],

$$\begin{aligned}(u_{C,j}^{ks})_t - \frac{4}{3}(u_{C,j}^{ks})_{x\bar{x}t} + \frac{1}{3}(u_{C,j}^{ks})_{\hat{x}\hat{x}t} + \frac{4}{3}(\rho_{C,j}^{ks+\frac{1}{2}})_{\hat{x}} - \frac{1}{3}(\rho_{C,j}^{ks+\frac{1}{2}})_{\ddot{x}} \\ + \frac{4}{9}\{u_{C,j}^{ks+\frac{1}{2}}(u_{C,j}^{ks+\frac{1}{2}})_{\hat{x}} + [(u_{C,j}^{ks+\frac{1}{2}})^2]_{\hat{x}}\} - \frac{1}{9}\{u_{C,j}^{ks+\frac{1}{2}}(u_{C,j}^{ks+\frac{1}{2}})_{\ddot{x}} + [(u_{C,j}^{ks+\frac{1}{2}})^2]_{\ddot{x}}\} = 0,\end{aligned} \tag{2}$$

$$(\rho_{C,j}^{ks})_t + \frac{4}{3}(u_{C,j}^{ks+\frac{1}{2}})_{\hat{x}} - \frac{1}{3}(u_{C,j}^{ks+\frac{1}{2}})_{\ddot{x}} = 0, \tag{3}$$

$$\begin{aligned}&u_{C,0}^{ks} = u_{C,J}^{ks} = 0, \quad \rho_{C,0}^{ks} = \rho_{C,J}^{ks} = 0, \quad 1 \leq k \leq P,\\ &u_{C,j}^{0} = u_0(x_L + jh), \quad \rho_{C,j}^{0} = \rho_0(x_L + jh), \quad 1 \leq j \leq J-1,\end{aligned}$$

where $u_{C,j}^{ks+\frac{1}{2}} = \frac{1}{2}(u_{C,j}^{(k+1)s} + u_{C,j}^{ks}), \rho_{C,j}^{ks+\frac{1}{2}} = \frac{1}{2}(\rho_{C,j}^{(k+1)s} + \rho_{C,j}^{ks})$.

Then, using the solutions u_C^{ks} and ρ_C^{ks} obtained at time levels t_{ks} from the initial step, we employ Lagrange's linear interpolation formula to calculate $u_C^{ks-l}, \rho_C^{ks-l}$ at time levels $t_{ks-l}(l = s-1, s-2, \ldots, 2, 1$ and $k = 1, 2, \ldots, P)$ and have

$$u_C^{ks-l} = \frac{t_{ks-l} - t_{ks}}{t_{(k-1)s} - t_{ks}} u_C^{(k-1)s} + \frac{t_{ks-l} - t_{(k-1)s}}{t_{ks} - t_{(k-1)s}} u_C^{ks} = \frac{l}{s} u_C^{(k-1)s} + (1 - \frac{l}{s}) u_C^{ks}, \tag{4}$$

$$\rho_C^{ks-l} = \frac{t_{ks-1} - t_{ks}}{t_{(k-1)s} - t_{ks}} \rho_C^{(k-1)s} + \frac{t_{ks-1} - t_{(k-1)s}}{t_{ks} - t_{(k-1)s}} \rho_C^{ks} = \frac{l}{s} \rho_C^{(k-1)s} + (1 - \frac{l}{s}) \rho_C^{ks}. \tag{5}$$

By following the previous two steps, we obtain all the numerical solutions $u_{C,j}^n$ and ρ_C^n $(n = 1, 2, \ldots, Ps = N, j = 1, 2, \ldots, J-1)$ on the fine time-mesh. It is important to note that the numerical solutions $u_{C,j}^n$ and ρ_C^n are only preliminary solutions and not the ultimate numerical solutions we aim to achieve for the SRLW equation.

Remark 1. *The solutions ρ_C^n are not essential for the subsequent step but are used for convergence and stability analysis of the proposed scheme.*

Next, we design a linear system on the fine time-mesh to obtain the final numerical solutions for the SRLW equation. Let $u_{F,j}^n = u(x_j, t_n), \rho_{F,j}^n = \rho(x_j, t_n)$ be the numerical solutions on the fine time-mesh, then similar to Equations (2) and (3), we obtain

$$\begin{aligned}(u_{F,j}^n)_t - \frac{4}{3}(u_{F,j}^n)_{x\bar{x}t} + \frac{1}{3}(u_{F,j}^n)_{\hat{x}\hat{x}t} + \frac{4}{3}(\rho_{F,j}^{n+\frac{1}{2}})_{\hat{x}} - \frac{1}{3}(\rho_{F,j}^{n+\frac{1}{2}})_{\ddot{x}} \\ + \frac{4}{9}\{u_{F,j}^{n+\frac{1}{2}}(u_{F,j}^{n+\frac{1}{2}})_{\hat{x}} + [(u_{F,j}^{n+\frac{1}{2}})^2]_{\hat{x}}\} - \frac{1}{9}\{u_{F,j}^{n+\frac{1}{2}}(u_{F,j}^{n+\frac{1}{2}})_{\ddot{x}} + [(u_{F,j}^{n+\frac{1}{2}})^2]_{\ddot{x}}\} = 0,\end{aligned} \tag{6}$$

$$(\rho_{F,j}^n)_t + \frac{4}{3}(u_{F,j}^{n+\frac{1}{2}})_{\hat{x}} - \frac{1}{3}(u_{F,j}^{n+\frac{1}{2}})_{\ddot{x}} = 0, \tag{7}$$

However, as we know, Equation (6) is still a nonlinear scheme. In order to construct the linear system, we use Taylor's formula to linearize the nonlinear terms of Equation (6) as follows. Using the notations in Section 2, we have

$$\begin{aligned}
&\frac{4}{9}\{u_{F,j}^{n+\frac{1}{2}}(u_{F,j}^{n+\frac{1}{2}})_{\hat{x}}+[(u_{F,j}^{n+\frac{1}{2}})^2]_{\hat{x}}\}-\frac{1}{9}\{u_{F,j}^{n+\frac{1}{2}}(u_{F,j}^{n+\frac{1}{2}})_{\ddot{x}}+[(u_{F,j}^{n+\frac{1}{2}})^2]_{\ddot{x}}\}\\
=&\frac{2}{9h}\{u_{F,j}^{n+\frac{1}{2}}(u_{F,j+1}^{n+\frac{1}{2}}-u_{F,j-1}^{n+\frac{1}{2}})+(u_{F,j+1}^{n+\frac{1}{2}})^2-(u_{F,j-1}^{n+\frac{1}{2}})^2\}\\
&-\frac{1}{36h}\{u_{F,j}^{n+\frac{1}{2}}(u_{F,j+2}^{n+\frac{1}{2}}-u_{F,j-2}^{n+\frac{1}{2}})+(u_{F,j+2}^{n+\frac{1}{2}})^2-(u_{F,j-2}^{n+\frac{1}{2}})^2\}\\
=&\frac{2}{9h}f(u_{F,j-1}^{n+\frac{1}{2}},u_{F,j}^{n+\frac{1}{2}},u_{F,j+1}^{n+\frac{1}{2}})-\frac{1}{36h}f(u_{F,j-2}^{n+\frac{1}{2}},u_{F,j}^{n+\frac{1}{2}},u_{F,j+2}^{n+\frac{1}{2}})
\end{aligned}\tag{8}$$

where $f(x,y,z)=(z-x)y+z^2-x^2$. Then, the Taylor's formula expansion is used to linearize the first part of Equation (8) at point $(u_{C,j-1}^{n+\frac{1}{2}},u_{C,j}^{n+\frac{1}{2}},u_{C,j+1}^{n+\frac{1}{2}})$ and the second part of Equation (8) at point $(u_{C,j-2}^{n+\frac{1}{2}},u_{C,j}^{n+\frac{1}{2}},u_{C,j+2}^{n+\frac{1}{2}})$, respectively, to obtain

$$\begin{aligned}
&f(u_{F,j-1}^{n+\frac{1}{2}},u_{F,j}^{n+\frac{1}{2}},u_{F,j+1}^{n+\frac{1}{2}})\\
&\approx f(u_{C,j-1}^{n+\frac{1}{2}},u_{C,j}^{n+\frac{1}{2}},u_{C,j+1}^{n+\frac{1}{2}})+f_x(u_{C,j-1}^{n+\frac{1}{2}},u_{C,j}^{n+\frac{1}{2}},u_{C,j+1}^{n+\frac{1}{2}})(u_{F,j-1}^{n+\frac{1}{2}}-u_{C,j-1}^{n+\frac{1}{2}})\\
&+f_y(u_{C,j-1}^{n+\frac{1}{2}},u_{C,j}^{n+\frac{1}{2}},u_{C,j+1}^{n+\frac{1}{2}})(u_{F,j}^{n+\frac{1}{2}}-u_{C,j}^{n+\frac{1}{2}})+f_z(u_{C,j-1}^{n+\frac{1}{2}},u_{C,j}^{n+\frac{1}{2}},u_{C,j+1}^{n+\frac{1}{2}})(u_{F,j+1}^{n+\frac{1}{2}}-u_{C,j+1}^{n+\frac{1}{2}})
\end{aligned}\tag{9}$$

and

$$\begin{aligned}
&f(u_{F,j-2}^{n+\frac{1}{2}},u_{F,j}^{n+\frac{1}{2}},u_{F,j+2}^{n+\frac{1}{2}})\\
&\approx f(u_{C,j-2}^{n+\frac{1}{2}},u_{C,j}^{n+\frac{1}{2}},u_{C,j+2}^{n+\frac{1}{2}})+f_x(u_{C,j-2}^{n+\frac{1}{2}},u_{C,j}^{n+\frac{1}{2}},u_{C,j+2}^{n+\frac{1}{2}})(u_{F,j-2}^{n+\frac{1}{2}}-u_{C,j-2}^{n+\frac{1}{2}})\\
&+f_y(u_{C,j-2}^{n+\frac{1}{2}},u_{C,j}^{n+\frac{1}{2}},u_{C,j+2}^{n+\frac{1}{2}})(u_{F,j}^{n+\frac{1}{2}}-u_{C,j}^{n+\frac{1}{2}})+f_z(u_{C,j-2}^{n+\frac{1}{2}},u_{C,j}^{n+\frac{1}{2}},u_{C,j+2}^{n+\frac{1}{2}})(u_{F,j+2}^{n+\frac{1}{2}}-u_{C,j+2}^{n+\frac{1}{2}})
\end{aligned}\tag{10}$$

Substituting Equations (8)–(10) into Equation (6) and denoting $f_j=f(u_{C,j-1}^{n+\frac{1}{2}},u_{C,j}^{n+\frac{1}{2}},u_{C,j+1}^{n+\frac{1}{2}})$, $f_{x,j}=f_x(u_{C,j-1}^{n+\frac{1}{2}},u_{C,j}^{n+\frac{1}{2}},u_{C,j+1}^{n+\frac{1}{2}})$, $f_{y,j}=f_y(u_{C,j-1}^{n+\frac{1}{2}},u_{C,j}^{n+\frac{1}{2}},u_{C,j+1}^{n+\frac{1}{2}})$, $f_{z,j}=f_z(u_{C,j-1}^{n+\frac{1}{2}},u_{C,j}^{n+\frac{1}{2}},u_{C,j+1}^{n+\frac{1}{2}})$, $\tilde{f}_j=f(u_{C,j-2}^{n+\frac{1}{2}},u_{C,j}^{n+\frac{1}{2}},u_{C,j+2}^{n+\frac{1}{2}})$, $\tilde{f}_{x,j}=f_x(u_{C,j-2}^{n+\frac{1}{2}},u_{C,j}^{n+\frac{1}{2}},u_{C,j+2}^{n+\frac{1}{2}})$, $\tilde{f}_{y,j}=f_y(u_{C,j-2}^{n+\frac{1}{2}},u_{C,j}^{n+\frac{1}{2}},u_{C,j+2}^{n+\frac{1}{2}})$, $\tilde{f}_{z,j}=f_z(u_{C,j-2}^{n+\frac{1}{2}},u_{C,j}^{n+\frac{1}{2}},u_{C,j+2}^{n+\frac{1}{2}})$, we construct a novel linear difference scheme that achieves a second-order convergence rate in time and a fourth-order convergence rate in space on the fine time-mesh as follows:

$$\begin{aligned}
&(u_{F,j}^{n})_t-\frac{4}{3}(u_{F,j}^{n})_{x\bar{x}t}+\frac{1}{3}(u_{F,j}^{n})_{\hat{x}\hat{x}t}+\frac{4}{3}(\rho_{F,j}^{n+\frac{1}{2}})_{\hat{x}}-\frac{1}{3}(\rho_{F,j}^{n+\frac{1}{2}})_{\ddot{x}}\\
&+\frac{2}{9h}\{f_j+f_{x,j}\cdot(u_{F,j-1}^{n+\frac{1}{2}}-u_{C,j-1}^{n+\frac{1}{2}})+f_{y,j}\cdot(u_{F,j}^{n+\frac{1}{2}}-u_{C,j}^{n+\frac{1}{2}})\\
&+f_{z,j}\cdot(u_{F,j+1}^{n+\frac{1}{2}}-u_{C,j+1}^{n+\frac{1}{2}})\}-\frac{1}{36h}\{\tilde{f}_j+\tilde{f}_{x,j}\cdot(u_{F,j-2}^{n+\frac{1}{2}}-u_{C,j-2}^{n+\frac{1}{2}})\\
&+\tilde{f}_{y,j}\cdot(u_{F,j}^{n+\frac{1}{2}}-u_{C,j}^{n+\frac{1}{2}})+\tilde{f}_{z,j}\cdot(u_{F,j+2}^{n+\frac{1}{2}}-u_{C,j+2}^{n+\frac{1}{2}})\}=0,
\end{aligned}\tag{11}$$

$$(\rho_{F,j}^{n})_t+\frac{4}{3}(u_{F,j}^{n+\frac{1}{2}})_{\hat{x}}-\frac{1}{3}(u_{F,j}^{n+\frac{1}{2}})_{\ddot{x}}=0,\tag{12}$$

$$\begin{aligned}
&u_{F,0}^{n}=u_{F,J}^{n}=0,\quad \rho_{F,0}^{n}=\rho_{F,J}^{n}=0,\quad 1\le n\le N,\\
&u_{F,j}^{0}=u_0(x_L+jh),\quad \rho_{F,j}^{0}=\rho_0(x_L+jh),\quad 1\le j\le J-1,
\end{aligned}$$

where

$$f_x(x,y,z) = -y - 2x, f_y(x,y,z) = z - x, f_z(x,y,z) = y + 2z$$

are the three partial derivatives of $f(x,y,z)$ with respect to x, y, z. The benefit of our method is that we avoid having to solve nonlinear equations at many time levels, and that instead, solve a much less expensive linear system.

Remark 2. *From Equation (11), one knows that the values u_F^n, u_C^n, u_C^{n+1} are utilized to obtain the u_F^{n+1}. However, similar to the Gauss–Seidel method applied to linear systems, our scheme has been modified by using u_F^n obtained from the previous time level instead of u_C^n in the calculation process to enhance the accuracy of the numerical solutions u_F^{n+1}.*

Remark 3. *The nonlinear system (2)–(3) is solved by Newton's method and when $|u_{F,j}^{n(k+1)} - u_{F,j}^{n(k)}| < 10^{-10}$, iteration stops, where k is the number of iterations. The linear system (11)–(12) is computed by a direct solver.*

4. The Convergence and Stability Analysis of the Scheme

In this section, we focus on conducting a convergence and stability analysis of scheme (2)–(5) on the coarse time-mesh and scheme (11)–(12) on the fine time-mesh. Let $v_j^n = u(x_j, t_n), \varphi_j^n = \rho(x_j, t_n)$ be the exact solutions of problem (1), then the truncation errors of the difference scheme (2)–(3) are obtained as follows:

$$\begin{aligned} Er_{C,j}^{ks} &= (v_j^{ks})_t - \frac{4}{3}(v_j^{ks})_{x\bar{x}t} + \frac{1}{3}(v_j^{ks})_{\hat{x}\hat{x}t} + \frac{4}{3}(\varphi_j^{ks+\frac{1}{2}})_{\hat{x}} - \frac{1}{3}(\varphi_j^{ks+\frac{1}{2}})_{\ddot{x}} \\ &+ \frac{4}{9}\{v_j^{ks+\frac{1}{2}}(v_j^{ks+\frac{1}{2}})_{\hat{x}} + [(v_j^{ks+\frac{1}{2}})^2]_{\hat{x}}\} - \frac{1}{9}\{v_j^{ks+\frac{1}{2}}(v_j^{ks+\frac{1}{2}})_{\ddot{x}} + [(v_j^{ks+\frac{1}{2}})^2]_{\ddot{x}}\}, \end{aligned} \tag{13}$$

$$Es_{C,j}^{ks} = (\varphi_j^{ks})_t + \frac{4}{3}(v_j^{ks+\frac{1}{2}})_{\hat{x}} - \frac{1}{3}(v_j^{ks+\frac{1}{2}})_{\ddot{x}}, \tag{14}$$

$$\begin{aligned} &v_0^{ks} = v_J^{ks} = 0, \varphi_0^{ks} = \varphi_J^{ks} = 0, \quad 1 \le k \le P, \\ &v_j^0 = v_0(x_L + jh), \varphi_j^0 = \varphi_0(x_L + jh), \quad 1 \le j \le J-1. \end{aligned}$$

By Taylor series expansion, we conclude

$$Er_{C,j}^{ks} = (u_t + \rho_x + uu_x - u_{xxt})_{(x_j,t_{ks})} + O(\tau_C^2 + h^4),$$

$$Es_{C,j}^{ks} = (\rho_t + u_x)_{(x_j,t_{ks})} + O(\tau_C^2 + h^4).$$

Theorem 1. *Suppose that $u_C^0 \in H_0^1[x_L, x_R], \rho_C^0 \in L_2[x_L, x_R]$, then the solutions of difference scheme (2)–(5) converge to the solutions of problem (1) with an order of $(\tau_C^2 + h^4)$ by the L_∞ norm for u_C^n and by the L_2 norm for ρ_C^n.*

Proof of Theorem 1. Denote $e_{C,j}^{ks} = v_j^{ks} - u_{C,j}^{ks}, \eta_{C,j}^{ks} = \varphi_j^{ks} - \rho_{C,j}^{ks}, 1 \le j \le J-1, 1 \le k \le P$. Subtracting Equation (2) from Equation (13), we obtain

$$\begin{aligned} Er_{C,j}^{ks} &= (e_{C,j}^{ks})_t - \frac{4}{3}(e_{C,j}^{ks})_{x\bar{x}t} + \frac{1}{3}(e_{C,j}^{ks})_{\hat{x}\hat{x}t} + \frac{4}{3}(\eta_{C,j}^{ks+\frac{1}{2}})_{\hat{x}} - \frac{1}{3}(\eta_{C,j}^{ks+\frac{1}{2}})_{\ddot{x}} \\ &+ \frac{4}{9}\{v_j^{ks+\frac{1}{2}}(v_j^{ks+\frac{1}{2}})_{\hat{x}} + [(v_j^{ks+\frac{1}{2}})^2]_{\hat{x}}\} - \frac{4}{9}\{u_{C,j}^{ks+\frac{1}{2}}(u_{C,j}^{ks+\frac{1}{2}})_{\hat{x}} + [(u_{C,j}^{ks+\frac{1}{2}})^2]_{\hat{x}}\} \\ &- \frac{1}{9}\{v_j^{ks+\frac{1}{2}}(v_j^{ks+\frac{1}{2}})_{\ddot{x}} + [(v_j^{ks+\frac{1}{2}})^2]_{\ddot{x}}\} + \frac{1}{9}\{u_{C,j}^{ks+\frac{1}{2}}(u_{C,j}^{ks+\frac{1}{2}})_{\ddot{x}} + [(u_{C,j}^{ks+\frac{1}{2}})^2]_{\ddot{x}}\}. \end{aligned} \tag{15}$$

Subtracting Equation (3) from Equation (14), we obtain

$$Es_{C,j}^{ks} = (\eta_{C,j}^{ks})_t + \frac{4}{3}(e_{C,j}^{ks+\frac{1}{2}})_{\hat{x}} - \frac{1}{3}(e_{C,j}^{ks+\frac{1}{2}})_{\ddot{x}}, \tag{16}$$

$$e_{C,j}^0 = 0, \quad \eta_{C,j}^0 = 0,$$
$$u_0^{ks} = u_J^{ks} = 0, \quad \rho_0^{ks} = \rho_J^{ks} = 0.$$

The following validation of the theorem consists of two situations: (i) We first prove the situation of $n = ks(k = 1, 2, \ldots, P)$; please refer to the references [16,27] for the proof of this part. In the end, we obtain

$$\|e_C^n\| \le O(\tau_C^2 + h^4), \quad \|e_{C,x}^n\| \le O(\tau_C^2 + h^4), \quad \|\eta_C^n\| \le O(\tau_C^2 + h^4). \tag{17}$$

From Lemma 4, we have

$$\|e_C^n\|_\infty \le O(\tau_C^2 + h^4); \tag{18}$$

(ii) Next, we prove the situation of $n = ks - l(l = s-1, s-2, \ldots, 2, 1$ and $k = 1, 2, \ldots, P)$. We use Lagrange's interpolation formula and obtain

$$\begin{aligned} v^{ks-l} &= \frac{t_{ks-l} - t_{ks}}{t_{(k-1)s} - t_{ks}} v^{(k-1)s} + \frac{t_{ks-l} - t_{(k-1)s}}{t_{ks} - t_{(k-1)s}} v^{ks} \\ &= \frac{l}{s} v^{(k-1)s} + (1 - \frac{l}{s}) v^{ks} + \frac{v''(\theta_1)}{2}(t - t_{(k-1)s})(t - t_{ks}), \quad \theta_1 \in (t_{(k-1)s}, t_{ks}), \end{aligned} \tag{19}$$

$$\begin{aligned} \varphi^{ks-l} &= \frac{t_{ks-l} - t_{ks}}{t_{(k-1)s} - t_{ks}} \varphi^{(k-1)s} + \frac{t_{ks-l} - t_{(k-1)s}}{t_{ks} - t_{(k-1)s}} \varphi^{ks} \\ &= \frac{l}{s} \varphi^{(k-1)s} + (1 - \frac{l}{s}) \varphi^{ks} + \frac{\varphi''(\theta_2)}{2}(t - t_{(k-1)s})(t - t_{ks}), \quad \theta_2 \in (t_{(k-1)s}, t_{ks}). \end{aligned} \tag{20}$$

Subtracting Equation (4) from Equation (19), we obtain

$$\begin{aligned} v^{ks-l} - u_C^{ks-l} =& \frac{l}{s}(v^{(k-1)s} - u_C^{(k-1)s}) + (1 - \frac{l}{s})(v^{ks} - u_C^{ks}) \\ &+ \frac{v''(\theta_1)}{2}(t - t_{(k-1)s})(t - t_{ks}). \end{aligned}$$

Subtracting Equation (5) from Equation (20), we obtain

$$\begin{aligned} \varphi^{ks-l} - \rho_C^{ks-l} =& \frac{l}{s}(\varphi^{(k-1)s} - \rho_C^{(k-1)s}) + (1 - \frac{l}{s})(\varphi^{ks} - \rho_C^{ks}) \\ &+ \frac{\varphi''(\theta_2)}{2}(t - t_{(k-1)s})(t - t_{ks}). \end{aligned}$$

From the triangle inequality and the results (17) and (18), we conclude

$$\|e_C^{ks-l}\| \le O(\tau_C^2 + h^4), \quad \|e_{C,x}^{ks-l}\| \le O(\tau_C^2 + h^4), \quad \|\eta_C^{ks-l}\| \le O(\tau_C^2 + h^4), \tag{21}$$

and

$$\|e_C^{ks-l}\|_\infty \le O(\tau_C^2 + h^4). \tag{22}$$

We derive the result of Theorem 1 by combining the two above-mentioned cases. □

Theorem 2. *Suppose that $u_C^0 \in H_0^1[x_L, x_R], \rho_C^0 \in L_2[x_L, x_R]$, then the solutions of difference scheme (2)–(5) are stable by the L_∞ norm for u_C^n and by the L_2 norm for ρ_C^n.*

Proof of Theorem 2. The theorem can be proved in the same way as that used to prove Theorem 1. □

Next, we analyze the convergence and stability of linear system (11) and (12) on the fine time-mesh. For simplification, we further denote $f_{xx,j} = f_{xx}(\xi_{j-1}, \varepsilon_j, \delta_{j+1})$, $f_{yy,j} = f_{yy}(\xi_{j-1}, \varepsilon_j, \delta_{j+1})$, $f_{zz,j} = f_{zz}(\xi_{j-1}, \varepsilon_j, \delta_{j+1})$, $\tilde{f}_{xx,j} = f_{xx}(\tilde{\xi}_{j-2}, \tilde{\varepsilon}_j, \tilde{\delta}_{j+2})$, $\tilde{f}_{yy,j} = f_{yy}(\tilde{\xi}_{j-2}, \tilde{\varepsilon}_j, \tilde{\delta}_{j+2})$, $\tilde{f}_{zz,j} = f_{zz}(\tilde{\xi}_{j-2}, \tilde{\varepsilon}_j, \tilde{\delta}_{j+2})$, $f_{xy,j} = f_{xy}(\xi_{j-1}, \varepsilon_j, \delta_{j+1})$, $f_{xz,j} = f_{xz}(\xi_{j-1}, \varepsilon_j, \delta_{j+1})$, $f_{yz,j} = f_{yz}(\xi_{j-1}, \varepsilon_j, \delta_{j+1})$, $\tilde{f}_{xy,j} = f_{xy}(\tilde{\xi}_{j-2}, \tilde{\varepsilon}_j, \tilde{\delta}_{j+2})$, $\tilde{f}_{xz,j} = f_{xz}(\tilde{\xi}_{j-2}, \tilde{\varepsilon}_j, \tilde{\delta}_{j+2})$, $\tilde{f}_{yz,j} = f_{yz}(\tilde{\xi}_{j-2}, \tilde{\varepsilon}_j, \tilde{\delta}_{j+2})$, where $f_{xx}(x,y,z) = -2$, $f_{yy}(x,y,z) = 0$, $f_{zz}(x,y,z) = 2$, $f_{xy}(x,y,z) = -1$, $f_{xz}(x,y,z) = 0$, $f_{yz}(x,y,z) = 1$ are the second-order partial derivatives of $f(x,y,z)$, $\xi_{j-1} \in (v^n_{j-1}, u^n_{C,j-1}), \varepsilon_j \in (v^n_j, u^n_{C,j}), \delta_{j+1} \in (v^n_{j+1}, u^n_{C,j+1})$, $\tilde{\xi}_{j-2} \in (v^n_{j-2}, u^n_{C,j-2}), \tilde{\varepsilon}_j \in (v^n_j, u^n_{C,j}), \tilde{\delta}_{j+2} \in (v^n_{j+2}, u^n_{C,j+2})$, then the truncation errors of the scheme (11)–(12) are obtained as follows:

$$
\begin{aligned}
Er^n_{F,j} &= (v^n_j)_t - \frac{4}{3}(v^n_j)_{x\bar{x}t} + \frac{1}{3}(v^n_j)_{\hat{x}\hat{x}t} + \frac{4}{3}(\varphi^{n+\frac{1}{2}}_j)_{\hat{x}} - \frac{1}{3}(\varphi^{n+\frac{1}{2}}_j)_{\ddot{x}} \\
&+ \frac{2}{9h}\{f_j + f_{x,j}\cdot(v^{n+\frac{1}{2}}_{j-1} - u^{n+\frac{1}{2}}_{C,j-1}) + f_{y,j}\cdot(v^{n+\frac{1}{2}}_j - u^{n+\frac{1}{2}}_{C,j}) + f_{z,j}\cdot(v^{n+\frac{1}{2}}_{j+1} - u^{n+\frac{1}{2}}_{C,j+1}) \\
&+ \frac{1}{2}f_{xx,j}\cdot(v^{n+\frac{1}{2}}_{j-1} - u^{n+\frac{1}{2}}_{C,j-1})^2 + \frac{1}{2}f_{yy,j}\cdot(v^{n+\frac{1}{2}}_j - u^{n+\frac{1}{2}}_{C,j})^2 + \frac{1}{2}f_{zz,j}\cdot(v^{n+\frac{1}{2}}_{j+1} - u^{n+\frac{1}{2}}_{C,j+1})^2 \\
&+ f_{xy,j}\cdot(v^{n+\frac{1}{2}}_{j-1} - u^{n+\frac{1}{2}}_{C,j-1})(v^{n+\frac{1}{2}}_j - u^{n+\frac{1}{2}}_{C,j}) + f_{xz,j}\cdot(v^{n+\frac{1}{2}}_{j-1} - u^{n+\frac{1}{2}}_{C,j-1})(v^{n+\frac{1}{2}}_{j+1} - u^{n+\frac{1}{2}}_{C,j+1}) \\
&+ f_{yz,j}\cdot(v^{n+\frac{1}{2}}_j - u^{n+\frac{1}{2}}_{C,j})(v^{n+\frac{1}{2}}_{j+1} - u^{n+\frac{1}{2}}_{C,j+1})\} \\
&- \frac{1}{36h}\{\tilde{f}_j + \tilde{f}_{x,j}\cdot(v^{n+\frac{1}{2}}_{j-2} - u^{n+\frac{1}{2}}_{C,j-2}) + \tilde{f}_{y,j}\cdot(v^{n+\frac{1}{2}}_j - u^{n+\frac{1}{2}}_{C,j}) + \tilde{f}_{z,j}\cdot(v^{n+\frac{1}{2}}_{j+2} - u^{n+\frac{1}{2}}_{C,j+2}) \\
&+ \frac{1}{2}\tilde{f}_{xx,j}\cdot(v^{n+\frac{1}{2}}_{j-2} - u^{n+\frac{1}{2}}_{C,j-2})^2 + \frac{1}{2}\tilde{f}_{yy,j}\cdot(v^{n+\frac{1}{2}}_j - u^{n+\frac{1}{2}}_{C,j})^2 + \frac{1}{2}\tilde{f}_{zz,j}\cdot(v^{n+\frac{1}{2}}_{j+2} - u^{n+\frac{1}{2}}_{C,j+2})^2 \\
&+ \tilde{f}_{xy,j}\cdot(v^{n+\frac{1}{2}}_{j-2} - u^{n+\frac{1}{2}}_{C,j-2})(v^{n+\frac{1}{2}}_j - u^{n+\frac{1}{2}}_{C,j}) + \tilde{f}_{xz,j}\cdot(v^{n+\frac{1}{2}}_{j-2} - u^{n+\frac{1}{2}}_{C,j-2})(v^{n+\frac{1}{2}}_{j+2} - u^{n+\frac{1}{2}}_{C,j+2}) \\
&+ \tilde{f}_{yz,j}\cdot(v^{n+\frac{1}{2}}_j - u^{n+\frac{1}{2}}_{C,j})(v^{n+\frac{1}{2}}_{j+2} - u^{n+\frac{1}{2}}_{C,j+2})\},
\end{aligned} \tag{23}
$$

$$
Es^n_{F,j} = (\varphi^n_j)_t + \frac{4}{3}(v^{n+\frac{1}{2}}_j)_{\hat{x}} - \frac{1}{3}(v^{n+\frac{1}{2}}_j)_{\ddot{x}}, \tag{24}
$$

$$
\begin{aligned}
&v^n_0 = v^n_J = 0, \quad \varphi^n_0 = \varphi^n_J = 0, \quad 1 \le n \le N, \\
&v^0_j = v_0(x_L + jh), \quad \varphi^0_j = \varphi_0(x_L + jh), \quad 1 \le j \le J-1.
\end{aligned}
$$

Theorem 3. *Suppose that $u^0_F \in H^1_0[x_L, x_R], \rho^0_F \in L_2[x_L, x_R]$, then the solutions of difference scheme (11)–(12) converge to the solutions of problem (1) with an order of $(\tau^2_F + \tau^4_C + h^4)$ by the L_∞ norm for u^n_F and by the L_2 norm for ρ^n_F.*

Proof of Theorem 3. Denote $e^n_{F,j} = v^n_j - u^n_{F,j}, \eta^n_{F,j} = \varphi^n_j - \rho^n_{F,j}, 1 \le j \le J-1, 1 \le n \le N$, Subtracting Equation (11) from Equation (23), we obtain

$$
\begin{aligned}
Er^n_{F,j} &= (e^n_{F,j})_t - \frac{4}{3}(e^n_{F,j})_{x\bar{x}t} + \frac{1}{3}(e^n_{F,j})_{\hat{x}\hat{x}t} + \frac{4}{3}(\eta^{n+\frac{1}{2}}_{F,j})_{\hat{x}} - \frac{1}{3}(\eta^{n+\frac{1}{2}}_{F,j})_{\ddot{x}} \\
&+ \frac{2}{9h}\{f_{x,j}\cdot e^{n+\frac{1}{2}}_{F,j-1} + f_{y,j}\cdot e^{n+\frac{1}{2}}_{F,j} + f_{z,j}\cdot e^{n+\frac{1}{2}}_{F,j+1} + Q_1\} \\
&- \frac{1}{36h}\{\tilde{f}_{x,j}\cdot e^{n+\frac{1}{2}}_{F,j-2} + \tilde{f}_{y,j}\cdot e^{n+\frac{1}{2}}_{F,j} + \tilde{f}_{z,j}\cdot e^{n+\frac{1}{2}}_{F,j+2} + Q_2\},
\end{aligned} \tag{25}
$$

where

$$
Q_1 = -(e^{n+\frac{1}{2}}_{C,j-1})^2 + (e^{n+\frac{1}{2}}_{C,j+1})^2 - (e^{n+\frac{1}{2}}_{C,j-1})(e^{n+\frac{1}{2}}_{C,j}) + (e^{n+\frac{1}{2}}_{C,j})(e^{n+\frac{1}{2}}_{C,j+1}),
$$

$$Q_2 = -(e_{C,j-2}^{n+\frac{1}{2}})^2 + (e_{C,j+2}^{n+\frac{1}{2}})^2 - (e_{C,j-2}^{n+\frac{1}{2}})(e_{C,j}^{n+\frac{1}{2}}) + (e_{C,j}^{n+\frac{1}{2}})(e_{C,j+2}^{n+\frac{1}{2}}).$$

Subtracting Equation (12) from Equation (24), we have

$$Es_{F,j}^n = (\eta_{F,j}^n)_t + \frac{4}{3}(e_{F,j}^{n+\frac{1}{2}})_{\hat{x}} - \frac{1}{3}(e_{F,j}^{n+\frac{1}{2}})_{\ddot{x}}. \tag{26}$$

Taking the inner product $(\cdot,\cdot)$ on both sides of Equation (25) with $2e_F^{n+\frac{1}{2}}$, we have

$$\begin{aligned}(Er_F^n, 2e_F^{n+\frac{1}{2}}) &= (e_{F,t}^n, 2e_F^{n+\frac{1}{2}}) - \frac{4}{3}(e_{F,x\bar{x}t}^n, 2e_F^{n+\frac{1}{2}}) + \frac{1}{3}(e_{F,\hat{x}\hat{x}t}^n, 2e_F^{n+\frac{1}{2}}) + \frac{8}{3}(\eta_{F,\hat{x}}^{n+\frac{1}{2}}, e_F^{n+\frac{1}{2}}) \\ &- \frac{2}{3}(\eta_{F,\ddot{x}}^{n+\frac{1}{2}}, e_F^{n+\frac{1}{2}}) + \frac{4}{9}\sum_{j=1}^{J-1}(f_{x,j}\cdot e_{F,j-1}^{n+\frac{1}{2}} + f_{y,j}\cdot e_{F,j}^{n+\frac{1}{2}} + f_{z,j}\cdot e_{F,j+1}^{n+\frac{1}{2}} + Q_1)e_{F,j}^{n+\frac{1}{2}} \\ &- \frac{1}{18}\sum_{j=1}^{J-1}(\tilde{f}_{x,j}\cdot e_{F,j-2}^{n+\frac{1}{2}} + \tilde{f}_{y,j}\cdot e_{F,j}^{n+\frac{1}{2}} + \tilde{f}_{z,j}\cdot e_{F,j+2}^{n+\frac{1}{2}} + Q_2)e_{F,j}^{n+\frac{1}{2}}.\end{aligned} \tag{27}$$

Notice that

$$(e_{F,t}^n, 2e_F^{n+\frac{1}{2}}) = \frac{1}{\tau_F}(\|e_F^{n+1}\|^2 - \|e_F^n\|^2), \tag{28}$$

$$(e_{F,x\bar{x}t}^n, 2e_F^{n+\frac{1}{2}}) = -\frac{1}{\tau_F}(\|e_{F,x}^{n+1}\|^2 - \|e_{F,x}^n\|^2), \tag{29}$$

$$(e_{F,\hat{x}xt}^n, 2e_F^{n+\frac{1}{2}}) = -\frac{1}{\tau_F}(\|e_{F,\hat{x}}^{n+1}\|^2 - \|e_{F,\hat{x}}^n\|^2), \tag{30}$$

$$(\eta_{F,\hat{x}}^{n+\frac{1}{2}}, e_F^{n+\frac{1}{2}}) = -(\eta_F^{n+\frac{1}{2}}, e_{F,\hat{x}}^{n+\frac{1}{2}}), \tag{31}$$

$$(\eta_{F,\ddot{x}}^{n+\frac{1}{2}}, e_F^{n+\frac{1}{2}}) = -(\eta_F^{n+\frac{1}{2}}, e_{F,\ddot{x}}^{n+\frac{1}{2}}), \tag{32}$$

$$(Er_F^n, 2e_F^{n+\frac{1}{2}}) \le \|Er_F^n\|^2 + \|e_F^{n+1}\|^2 + \|e_F^n\|^2. \tag{33}$$

Furthermore, from Lemmas 1 and 2, Lemma 4.2 in [16], and the Cauchy–Schwarz inequality, we have

$$\begin{aligned}&\sum_{j=1}^{J-1}(f_{x,j}\cdot e_{F,j-1}^{n+\frac{1}{2}} + f_{y,j}\cdot e_{F,j}^{n+\frac{1}{2}} + f_{z,j}\cdot e_{F,j+1}^{n+\frac{1}{2}})e_{F,j}^{n+\frac{1}{2}} \\ &= h\sum_{j=1}^{J-1}[-f_{x,j}\cdot(e_{F,j}^{n+\frac{1}{2}})_{\bar{x}} + \frac{3}{h}f_{y,j}\cdot e_{F,j}^{n+\frac{1}{2}} + f_{z,j}\cdot(e_{F,j}^{n+\frac{1}{2}})_x]e_{F,j}^{n+\frac{1}{2}} \\ &= -(\boldsymbol{f}_x\cdot e_{F,\bar{x}}^{n+\frac{1}{2}}, e_F^{n+\frac{1}{2}}) + \frac{3}{h}(\boldsymbol{f}_y\cdot e_F^{n+\frac{1}{2}}, e_F^{n+\frac{1}{2}}) + (\boldsymbol{f}_z\cdot e_{F,x}^{n+\frac{1}{2}}, e_F^{n+\frac{1}{2}}) \\ &\le M(\|e_{F,x}^{n+\frac{1}{2}}\|^2 + \|e_F^{n+\frac{1}{2}}\|^2),\end{aligned} \tag{34}$$

$$\begin{aligned}\sum_{j=1}^{J-1}Q_1 e_{F,j}^{n+\frac{1}{2}} &= 2h\sum_{j=1}^{J-1}(e_{C,j}^{n+\frac{1}{2}})_{\hat{x}}^2 e_{F,j}^{n+\frac{1}{2}} + 2h\sum_{j=1}^{J-1}(e_{C,j}^{n+\frac{1}{2}})_{\hat{x}} e_{C,j}^{n+\frac{1}{2}} e_{F,j}^{n+\frac{1}{2}} \\ &= 2((e_C^{n+\frac{1}{2}})_{\hat{x}}^2, e_F^{n+\frac{1}{2}}) + 2(e_{C,\hat{x}}^{n+\frac{1}{2}} e_C^{n+\frac{1}{2}}, e_F^{n+\frac{1}{2}}) \\ &\le M(\|e_C^{n+\frac{1}{2}}\|_\infty^2\|e_C^{n+\frac{1}{2}}\|^2 + \|e_C^{n+\frac{1}{2}}\|_\infty^2\|e_{C,x}^{n+\frac{1}{2}}\|^2 + \|e_{F,x}^{n+\frac{1}{2}}\|^2 + \|e_F^{n+\frac{1}{2}}\|^2),\end{aligned} \tag{35}$$

$$
\begin{aligned}
&\sum_{j=1}^{J-1}(\tilde{f}_{x,j}\cdot e_{F,j-2}^{n+\frac{1}{2}}+\tilde{f}_{y,j}\cdot e_{F,j}^{n+\frac{1}{2}}+\tilde{f}_{z,j}\cdot e_{F,j+2}^{n+\frac{1}{2}})e_{F,j}^{n+\frac{1}{2}}\\
&=h\sum_{j=1}^{J-1}[-\tilde{f}_{x,j}\cdot(e_{F,j-1}^{n+\frac{1}{2}})_{\bar{x}}+\tilde{f}_{z,j}\cdot(e_{F,j+1}^{n+\frac{1}{2}})_{x}]e_{F,j}^{n+\frac{1}{2}}\\
&+\sum_{j=1}^{J-1}(\tilde{f}_{x,j}\cdot e_{F,j-1}^{n+\frac{1}{2}}+\tilde{f}_{y,j}\cdot e_{F,j}^{n+\frac{1}{2}}+\tilde{f}_{z,j}\cdot e_{F,j+1}^{n+\frac{1}{2}})e_{F,j}^{n+\frac{1}{2}}\\
&=h^2\sum_{j=1}^{J+1}\tilde{f}_{x,j}\cdot(e_{F,j}^{n+\frac{1}{2}})_{\bar{x}\bar{x}}e_{F,j}^{n+\frac{1}{2}}-h\sum_{j=1}^{J-1}\tilde{f}_{x,j}\cdot(e_{F,j}^{n+\frac{1}{2}})_{\bar{x}}e_{F,j}^{n+\frac{1}{2}}+h^2\sum_{j=1}^{J-1}\tilde{f}_{z,j}\cdot(e_{F,j}^{n+\frac{1}{2}})_{xx}e_{F,j}^{n+\frac{1}{2}}\\
&+h\sum_{j=1}^{J-1}\tilde{f}_{z,j}\cdot(e_{F,j}^{n+\frac{1}{2}})_{x}e_{F,j}^{n+\frac{1}{2}}-(\tilde{f}_{x}\cdot e_{F,\bar{x}}^{n+\frac{1}{2}},e_{F}^{n+\frac{1}{2}})+\frac{3}{h}(\tilde{f}_{y}\cdot e_{F}^{n+\frac{1}{2}},e_{F}^{n+\frac{1}{2}})+(\tilde{f}_{z}\cdot e_{F,x}^{n+\frac{1}{2}},e_{F}^{n+\frac{1}{2}})\\
&=h(\tilde{f}_{x}\cdot e_{F,\frac{1}{2}}^{n+\frac{1}{2}}e_{F}^{n+\frac{1}{2}})+h(\tilde{f}_{z}\cdot e_{F,xx}^{n+\frac{1}{2}},e_{F}^{n+\frac{1}{2}})-2(\tilde{f}_{x}\cdot e_{F,\bar{x}}^{n+\frac{1}{2}},e_{F}^{n+\frac{1}{2}})\\
&+\frac{3}{h}(\tilde{f}_{y}\cdot e_{F}^{n+\frac{1}{2}},e_{F}^{n+\frac{1}{2}})+2(\tilde{f}_{z}\cdot e_{F,x}^{n+\frac{1}{2}},e_{F}^{n+\frac{1}{2}})\\
&\le M(\|e_{F,x}^{n+\frac{1}{2}}\|^2+\|e_{F}^{n+\frac{1}{2}}\|^2),
\end{aligned}
\tag{36}
$$

$$
\begin{aligned}
\sum_{j=1}^{J-1}Q_2e_{F,j}^{n+\frac{1}{2}}&=4h\sum_{j=1}^{J-1}(e_{C,j}^{n+\frac{1}{2}})_{\ddot{x}}^2e_{F,j}^{n+\frac{1}{2}}+4h\sum_{j=1}^{J-1}(e_{C,j}^{n+\frac{1}{2}})_{\ddot{x}}e_{C,j}^{n+\frac{1}{2}}e_{F,j}^{n+\frac{1}{2}}\\
&=4((e_{C}^{n+\frac{1}{2}})_{\ddot{x}}^2,e_{F}^{n+\frac{1}{2}})+4(e_{C,\ddot{x}}^{n+\frac{1}{2}}e_{C}^{n+\frac{1}{2}},e_{F}^{n+\frac{1}{2}})\\
&\le M(\|e_{C}^{n+\frac{1}{2}}\|_\infty^2\|e_{C}^{n+\frac{1}{2}}\|^2+\|e_{C}^{n+\frac{1}{2}}\|_\infty^2\|e_{C,x}^{n+\frac{1}{2}}\|^2+\|e_{F,x}^{n+\frac{1}{2}}\|^2+\|e_{F}^{n+\frac{1}{2}}\|^2).
\end{aligned}
\tag{37}
$$

Substituting Equations (28)–(37) into Equation (27), then

$$
\begin{aligned}
&\|e_F^{n+1}\|^2+\frac{4}{3}\|e_{F,x}^{n+1}\|^2-\frac{1}{3}\|e_{F,\hat{x}}^{n+1}\|^2-\frac{8\tau_F}{3}(\eta_F^{n+\frac{1}{2}},e_{F,\hat{x}}^{n+\frac{1}{2}})+\frac{2\tau_F}{3}(\eta_F^{n+\frac{1}{2}},e_{F,\ddot{x}}^{n+\frac{1}{2}})\\
&\le\|e_F^{n}\|^2+\frac{4}{3}\|e_{F,x}^{n}\|^2-\frac{1}{3}\|e_{F,\hat{x}}^{n}\|^2+M\tau_F(\|e_F^{n+1}\|^2+\|e_F^{n}\|^2+\|e_{F,x}^{n+1}\|^2+\|e_{F,x}^{n}\|^2)\\
&\quad+M\tau_F(\|e_C^{n+\frac{1}{2}}\|_\infty^2\|e_C^{n+\frac{1}{2}}\|^2+\|e_C^{n+\frac{1}{2}}\|_\infty^2\|e_{C,x}^{n+\frac{1}{2}}\|^2)+\tau_F\|Er_F^n\|^2.
\end{aligned}
\tag{38}
$$

Taking the inner product $(\cdot,\cdot)$ on both sides of Equation (26) with $2\eta_F^{n+\frac{1}{2}}$, we obtain

$$
(Es_{F,j}^n,2\eta_F^{n+\frac{1}{2}})=(\eta_{F,t}^n,2\eta_F^{n+\frac{1}{2}})+\frac{8}{3}(e_{F,\hat{x}}^{n+\frac{1}{2}},\eta_F^{n+\frac{1}{2}})-\frac{2}{3}(e_{F,\ddot{x}}^{n+\frac{1}{2}},\eta_F^{n+\frac{1}{2}}).
\tag{39}
$$

We also have

$$
(\eta_{F,t}^n,2\eta_F^{n+\frac{1}{2}})=\frac{1}{\tau_F}(\|\eta_F^{n+1}\|^2-\|\eta_F^{n}\|^2),
\tag{40}
$$

$$
(Es_{F,j}^n,2\eta_F^{n+\frac{1}{2}})\le\|Es_F^n\|^2+\|\eta_F^{n+1}\|^2+\|\eta_F^{n}\|^2.
\tag{41}
$$

Substituting Equations (40) and (41) into Equation (39), then

$$
\begin{aligned}
&\|\eta_F^{n+1}\|^2+\frac{8\tau_F}{3}(e_{F,\hat{x}}^{n+\frac{1}{2}},\eta_F^{n+\frac{1}{2}})-\frac{2\tau_F}{3}(e_{F,\ddot{x}}^{n+\frac{1}{2}},\eta_F^{n+\frac{1}{2}})\\
&\le\|\eta_F^{n}\|^2+M\tau_F(\|\eta_F^{n+1}\|^2+\|\eta_F^{n}\|^2)+\tau_F\|Es_F^n\|^2.
\end{aligned}
\tag{42}
$$

Adding Equations (38) and (42), we have

$$\begin{aligned}
&\|e_F^{n+1}\|^2+\frac{4}{3}\|e_{F,x}^{n+1}\|^2-\frac{1}{3}\|e_{F,\hat{x}}^{n+1}\|^2+\|\eta_F^{n+1}\|^2\\
&\le \|e_F^{n}\|^2+\frac{4}{3}\|e_{F,x}^{n}\|^2-\frac{1}{3}\|e_{F,\hat{x}}^{n}\|^2+\|\eta_F^{n}\|^2\\
&\quad+M\tau_F(\|e_F^{n+1}\|^2+\|e_F^{n}\|^2+\|e_{F,x}^{n+1}\|^2+\|e_{F,x}^{n}\|^2+\|\eta_F^{n+1}\|^2+\|\eta_F^{n}\|^2)\\
&\quad+M\tau_F(\|e_C^{n+\frac{1}{2}}\|_\infty^2\|e_C^{n+\frac{1}{2}}\|^2+\|e_C^{n+\frac{1}{2}}\|_\infty^2\|e_{C,x}^{n+\frac{1}{2}}\|^2)+\tau_F\|Er_F^n\|^2+\tau_F\|Es_F^n\|^2.
\end{aligned}\tag{43}$$

Let $B_F^n=\|e_F^n\|^2+\frac{4}{3}\|e_{F,x}^n\|^2-\frac{1}{3}\|e_{F,\hat{x}}^n\|^2+\|\eta_F^n\|^2$, then

$$\begin{aligned}
B_F^{n+1}-B_F^n\le M\tau_F(B_F^{n+1}+B_F^n)+M\tau_F(\|e_C^{n+\frac{1}{2}}\|_\infty^2\|e_C^{n+\frac{1}{2}}\|^2+\|e_C^{n+\frac{1}{2}}\|_\infty^2\|e_{C,x}^{n+\frac{1}{2}}\|^2)\\
+\tau_F\|Er_F^n\|^2+\tau_F\|Es_F^n\|^2.
\end{aligned}$$

By using the result of the Theorem 1, we obtain

$$(1-M\tau_F)(B_F^{n+1}-B_F^n)\le 2M\tau_F B_F^n+M\tau_F(\tau_F^4+\tau_C^8+h^8).$$

Choosing τ_F to be sufficiently small such that $(1-M\tau_F)>\lambda>0$, then

$$B_F^{n+1}-B_F^n\le M\tau_F(\tau_F^4+\tau_C^8+h^8)+M\tau_F B_F^n.\tag{44}$$

Summing the inequalities in Equation (44) from 0 to $N-1$, we obtain

$$B_F^N\le B_F^0+M(\tau_F^4+\tau_C^8+h^8)+M\tau_F\sum_{n=0}^{N-1}B_F^n.$$

From Lemma 3, we have

$$B_F^N\le[B_F^0+M(\tau_F^4+\tau_C^8+h^8)]e^{MN\tau_F}.\tag{45}$$

Using the initial and boundary conditions, we get following results from Equation (45)

$$\|e_F^n\|\le O(\tau_F^2+\tau_C^4+h^4),\|e_{F,x}^n\|\le O(\tau_F^2+\tau_C^4+h^4),\|\eta_F^n\|<O(\tau_F^2+\tau_C^4+h^4).$$

Using Lemma 4, this leads to

$$\|e_F^n\|_\infty\le O(\tau_F^2+\tau_C^4+h^4).$$

This completes the proof of the Theorem. □

Theorem 4. *Suppose that $u_F^0\in H_0^1[x_L,x_R],\rho_F^0\in L_2[x_L,x_R]$, then the solutions of difference scheme (11)–(12) are stable by the L_∞ norm for u_F^n and by the L_2 norm for ρ_F^n.*

Proof of Theorem 4. The way used to prove Theorem 3 can also be applied to demonstrate the validity of this theorem. □

5. Numerical Simulation Results

In this section, we conducted several numerical simulations of the proposed scheme for solving the SRLW equation. On the one hand, we present the computational efficiency and numerical accuracy of the proposed scheme and compare the obtained results with the nonlinear scheme in [16] and the TT-M difference scheme in [27], respectively. On the other hand, we focus on the conservation laws and the long-time behavior simulation of the proposed scheme. All simulations are implemented on a personal computer running Windows 10 with an Intel(R) i7-10710U 1.61 GHz CPU and 16 GB of memory using Matlab R2019b.

For all experiments, we selected the following domains and parameters: $-50 \leq x \leq 50$, $0 < t \leq 10$, and $s = 4, m = 1.5$. The SRLW equation possesses the following solitary wave solution

$$u(x,t) = \frac{3(m^2-1)}{m}\operatorname{sech}^2\left(\sqrt{\frac{m^2-1}{4v^2}}(x-mt)\right),$$
$$\rho(x,t) = \frac{3(m^2-1)}{m^2}\operatorname{sech}^2\left(\sqrt{\frac{m^2-1}{4m^2}}(x-mt)\right),$$

and

$$u_0(x) = \frac{5}{2}\operatorname{sech}^2\frac{\sqrt{5}}{6}x, \quad \rho_0(x) = \frac{5}{3}\operatorname{sech}^2\frac{\sqrt{5}}{6}x.$$

The error and convergence rate of the numerical solutions with respect to the exact velocity v and density φ are defined as follows:

$$e(h,\tau) = \|v^n - u^n\|_\infty, \ \ \eta(h,\tau) = \|\varphi^n - \rho^n\|,$$
$$uRate_x = \log_2\left(\frac{e(2h,4\tau)}{e(h,\tau)}\right), \ \rho Rate_x = \log_2\left(\frac{\eta(2h,4\tau)}{\eta(h,\tau)}\right),$$
$$uRate_t = \log_2\left(\frac{e(2h,2\tau)}{e(h,\tau)}\right), \ \rho Rate_t = \log_2\left(\frac{\eta(2h,2\tau)}{\eta(h,\tau)}\right).$$

First, we verify that the proposed scheme can achieve second-order convergence in time and fourth-order convergence in space. To do so, we obtain the errors between the numerical and exact solution at $t = 10$ with various time and space steps. The convergence rates and CPU times determined by both the nonlinear scheme in [16] and the proposed scheme are summarized in Tables 1 and 2. From the results presented the tables, we can see that: (i) the errors provided by the proposed scheme are nearly identical to those obtained from the nonlinear scheme; (ii) Both schemes exhibit approximately second-order convergence in time when $h = \tau_F$ and fourth-order convergence in space when $\tau_F = h^2$. These results verify the analysis results stated in Theorem 3; however, (iii) The proposed scheme is significantly more cost-effective than the nonlinear scheme. In other words, the CPU time required by the proposed scheme is approximately half that needed by the nonlinear scheme. The results in Tables 1 and 2 clearly demonstrate that a significant improvement has been achieved by proposed scheme compared to the nonlinear scheme in [16].

Table 1. The errors and convergence rates with $\tau_F = h^2$.

Nonlinear Scheme [16]					
(h, τ_F)	$e(h, \tau_F)$	$uRate_x$	$\eta(h, \tau_F)$	$\rho Rate_x$	**CPU(s)**
$\left(\frac{1}{2}, \frac{1}{4}\right)$	6.0793×10^{-2}	—	8.4371×10^{-2}	—	1.83
$\left(\frac{1}{4}, \frac{1}{16}\right)$	3.9382×10^{-3}	3.9482	5.4315×10^{-3}	3.9573	17.30
$\left(\frac{1}{8}, \frac{1}{64}\right)$	2.4688×10^{-4}	3.9956	3.4032×10^{-4}	3.9963	283.50
$\left(\frac{1}{16}, \frac{1}{256}\right)$	1.5452×10^{-5}	3.9979	2.1277×10^{-5}	3.9995	5664.93
Proposed Scheme					
(h, τ_F)	$e(h, \tau_F)$	$uRate_x$	$\eta(h, \tau_F)$	$\rho Rate_x$	**CPU(s)**
$\left(\frac{1}{2}, \frac{1}{4}\right)$	7.5147×10^{-2}	—	1.0501×10^{-1}	—	1.00
$\left(\frac{1}{4}, \frac{1}{16}\right)$	3.9370×10^{-3}	4.2545	5.5879×10^{-3}	4.2320	9.57
$\left(\frac{1}{8}, \frac{1}{64}\right)$	2.4687×10^{-4}	3.9952	3.4096×10^{-4}	4.0346	142.86
$\left(\frac{1}{16}, \frac{1}{256}\right)$	1.5452×10^{-5}	3.9978	2.1279×10^{-5}	4.0021	2956.44

Table 2. The errors and convergence rates with $h = \tau_F$.

Nonlinear Scheme [16]					
(h, τ_F)	$e(h, \tau_F)$	$uRate_t$	$\eta(h, \tau_F)$	$\rho Rate_t$	**CPU(s)**
$\left(\frac{1}{4}, \frac{1}{4}\right)$	5.5120×10^{-2}	—	7.6668×10^{-2}	—	6.47
$\left(\frac{1}{8}, \frac{1}{8}\right)$	1.3991×10^{-2}	1.9780	1.9390×10^{-2}	1.9833	62.37
$\left(\frac{1}{16}, \frac{1}{16}\right)$	3.5125×10^{-3}	1.9939	4.8616×10^{-3}	1.9958	459.76
$\left(\frac{1}{32}, \frac{1}{32}\right)$	8.7882×10^{-4}	1.9988	1.2162×10^{-3}	1.9990	5357.84
Proposed Scheme					
(h, τ_F)	$e(h, \tau_F)$	$uRate_t$	$\eta(h, \tau_F)$	$\rho Rate_t$	**CPU(s)**
$\left(\frac{1}{4}, \frac{1}{4}\right)$	7.2702×10^{-2}	—	9.8577×10^{-2}	—	3.06
$\left(\frac{1}{8}, \frac{1}{8}\right)$	1.4349×10^{-2}	2.3410	2.1666×10^{-2}	2.1858	23.59
$\left(\frac{1}{16}, \frac{1}{16}\right)$	3.5100×10^{-3}	2.0314	5.0243×10^{-3}	2.1084	206.61
$\left(\frac{1}{32}, \frac{1}{32}\right)$	8.7874×10^{-4}	1.9979	1.2267×10^{-3}	2.0341	2472.98

The three-dimensional plots of the numerical solutions of $u(x,t)$ and $\rho(x,t)$ for problem (1) using the proposed scheme by taking $h = 1/8$ and $\tau_F = 1/64$ are presented in Figure 1. These visualizations provide insights into the evolution of wave propagation over the time interval $[0, 10]$. Additionally, Figure 2 shows the exact and numerical solutions of $u(x,t)$ and $\rho(x,t)$ with $h = 1/8$ and $\tau_F = 1/64$ at $t = 10$ obtained from the proposed scheme. A comparison clearly illustrates a remarkable agreement between our numerical solutions and the exact solution. Moreover, Figure 3 displays the computational times (CPU times) required by the nonlinear scheme in [16] and the proposed scheme for different choices of $\tau_F = h^2$ and $h = \tau_F$. Notably, our proposed scheme demonstrates a large reduction in computation time. In conclusion, in contrast to the nonlinear method presented in [16], the proposed scheme not only preserves nearly the same accuracy and convergence rate as the nonlinear scheme but also substantially decreases the CPU time needed to obtain numerical solutions.

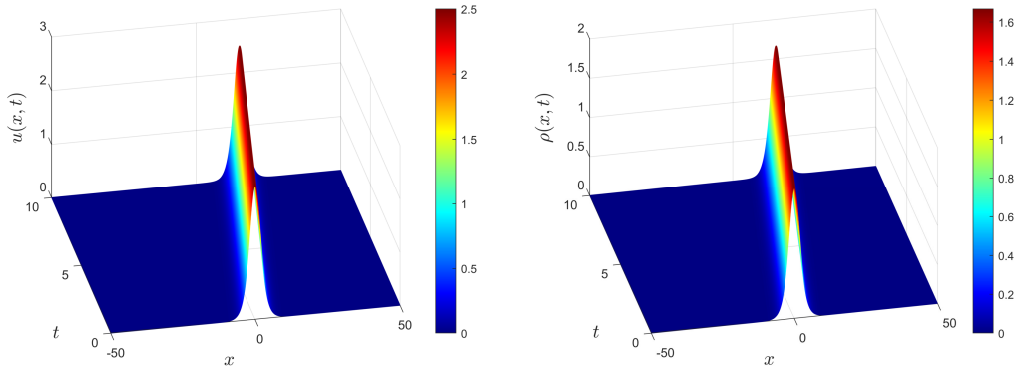

(**a**) (**b**)

Figure 1. Three−dimensional plots of $u(x,t)$ (**a**) and $\rho(x,t)$ (**b**) with $h = 1/8$, $\tau_F = 1/64$.

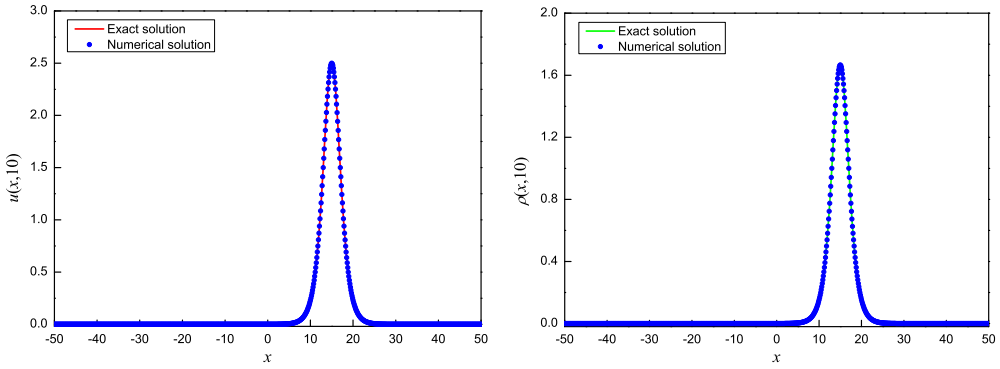

(**a**) (**b**)

Figure 2. Exact and numerical solution of $u(x,t)$ (**a**) and $\rho(x,t)$ (**b**) at $t = 10$ with $h = 1/8, \tau_F = 1/64$.

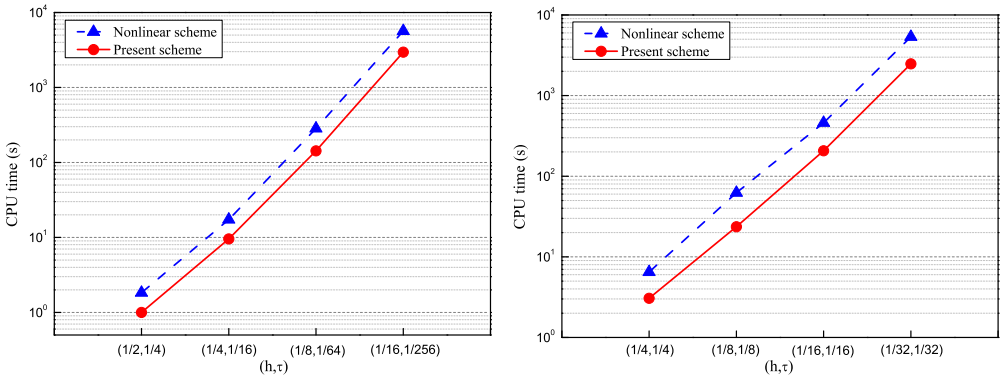

(**a**) (**b**)

Figure 3. Comparison of CPU times with $\tau_F = h^2$ (**a**) and $h = \tau_F$ (**b**).

Next, we compare the accuracy of two schemes for the SRLW equation: the previous TT-M scheme in [27] and the proposed scheme. The former scheme exhibits first-order convergence in time and second-order convergence in space. Under the same temporal and spatial domain conditions as in this article, we use the previous TT-M scheme to calculate the errors of $u(x,t)$ and $\rho(x,t)$ as well as the CPU time for different time and space steps. The resulting data are presented in Table 3. By comparing the errors and CPU times presented in Tables 1–3, it is evident that the proposed scheme exhibits significantly lower CPU time requirements compared to that of the previous TT-M scheme under similar error value. This indicates that the computational efficiency of the proposed scheme is higher than that of the previous TT-M scheme. Figures 4 and 5 illustrate the error comparison between the two methods with $h = 1/8, \tau_F = 1/64$ and $h = 1/16, \tau_F = 1/16$, respectively. The results show that the errors in numerical solutions of $u(x,t)$ and $\rho(x,t)$ obtained from the proposed scheme are considerably smaller than the errors provided by the previous TT-M scheme, which implies that our proposed method has superior accuracy than the previous TT-M scheme for solving the SRLW equation.

Furthermore, based on Tables 1–3, we present the errors of $u(x,t)$ and $\rho(x,t)$ versus the CPU time using the three numerical schemes (i.e., nonlinear scheme, previous TT-M scheme and proposed scheme) in Figure 6. Figure 6 plots the errors versus the CPU time under $\tau_F = h^2$ and $h = \tau_F$, respectively. From the figure, one can see that the cost of the previous TT-M scheme is the most expensive; the cost of the proposed scheme is the cheapest; and the cost of the nonlinear scheme is more expensive than that provided by the proposed scheme.

Table 3. The errors and CPU times of the previous TT-M scheme with various time and space steps.

Previous TT-M Scheme [27]			
(h, τ_F)	$e(h, \tau_F)$	$\eta(h, \tau_F)$	**CPU(s)**
$\left(\frac{1}{2}, \frac{1}{4}\right)$	7.7523×10^{-1}	7.6225×10^{-1}	0.18
$\left(\frac{1}{4}, \frac{1}{16}\right)$	1.7627×10^{-1}	1.7062×10^{-1}	1.90
$\left(\frac{1}{8}, \frac{1}{64}\right)$	4.2888×10^{-2}	4.1560×10^{-2}	26.32
$\left(\frac{1}{16}, \frac{1}{256}\right)$	1.0658×10^{-2}	1.0324×10^{-2}	366.92
$\left(\frac{1}{4}, \frac{1}{4}\right)$	8.9609×10^{-1}	8.2590×10^{-1}	1.01
$\left(\frac{1}{8}, \frac{1}{8}\right)$	4.1952×10^{-1}	3.9001×10^{-1}	5.40
$\left(\frac{1}{16}, \frac{1}{16}\right)$	2.0123×10^{-1}	1.8915×10^{-1}	31.49
$\left(\frac{1}{32}, \frac{1}{32}\right)$	9.8428×10^{-2}	9.3111×10^{-2}	240.06

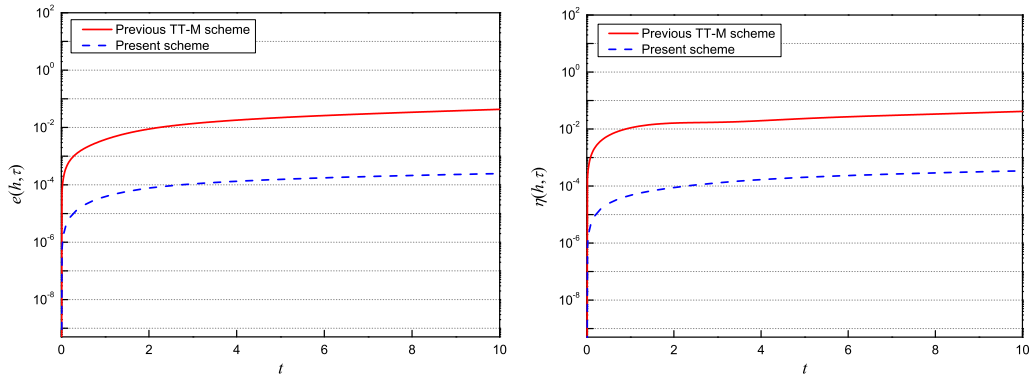

(**a**) (**b**)

Figure 4. Comparison of $e(h, \tau_F)$ (**a**) and $\eta(h, \tau_F)$ (**b**) with $h = 1/8, \tau_F = 1/64$.

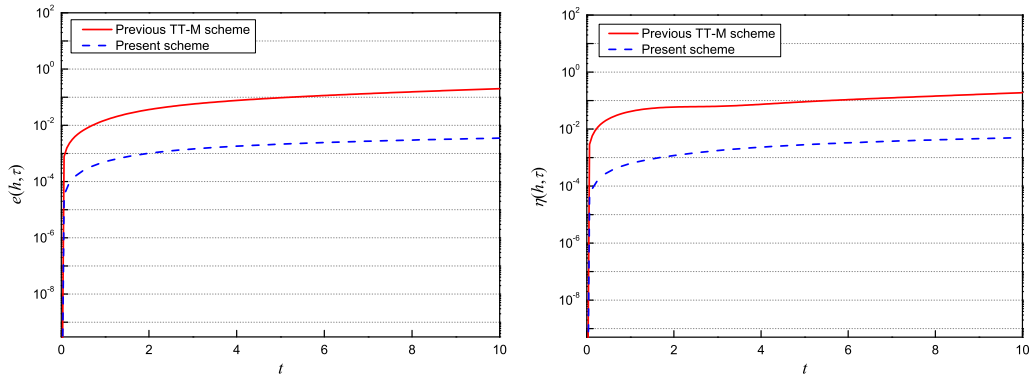

(**a**) (**b**)

Figure 5. Comparison of $e(h, \tau_F)$ (**a**) and $\eta(h, \tau_F)$ (**b**) with $h = 1/16, \tau_F = 1/16$.

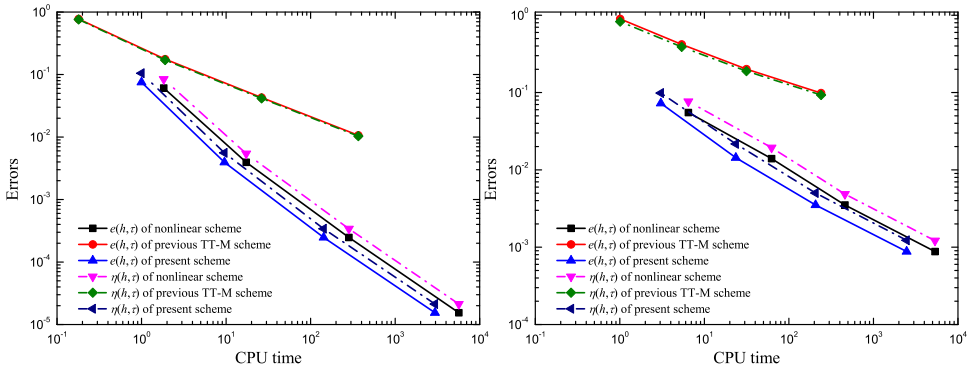

Figure 6. The numerical error versus the CPU time using the three different numerical schemes with $\tau_F = h^2$ (**a**) and $h = \tau_F$ (**b**).

Next, we consider the three conservation laws of the SRLW Equation (1), namely:

$$Q_1(t) = \int_{-\infty}^{\infty} u(x,t)dx, \quad Q_2(t) = \int_{-\infty}^{\infty} \rho(x,t)dx, \quad E(t) = \|u\|^2 + \|u_x\|^2 + \|\rho\|^2.$$

Subsequently, by utilizing discretized formulations, we are able to evaluate three approximate conservative quantities as follows:

$$Q_1 = h\sum_{j=1}^{J-1} u_j^n, \quad Q_2 = h\sum_{j=1}^{J-1} \rho_j^n, \quad E = h\sum_{j=1}^{J-1}(u_j^n)^2 + \frac{1}{h}\sum_{j=1}^{J-1}(u_{j+1}^n - u_j^n)^2 + h\sum_{j=1}^{J-1}(\rho_j^n)^2,$$

where $n = 0, 1, 2, \ldots, N$.

The values of these three quantities under different time and spatial steps are recorded in Tables 4–6. Tables 4 and 5 demonstrate that the discrete masses Q_1 and Q_2 remain well-preserved at various times, regardless of the time and space steps. From the results presented in Table 6, for the case where the grid spacing is $h = 1/2$ and the time step is $\tau_F = 1/4$, it can be observed that the discrete energy E undergoes a slight change over time. However, as the spatial and temporal step sizes become smaller, the tables show that our proposed scheme preserves the two discrete masses well and almost maintains discrete energy when the time and space steps are made smaller.

Table 4. Discrete mass Q_1 under different mesh steps h and τ_F at various times.

Present Scheme				
	$\left(\frac{1}{2}, \frac{1}{4}\right)$	$\left(\frac{1}{4}, \frac{1}{16}\right)$	$\left(\frac{1}{8}, \frac{1}{64}\right)$	$\left(\frac{1}{16}, \frac{1}{256}\right)$
$t = 0$	13.4164078649	13.4164078649	13.4164078649	13.4164078649
$t = 2$	13.4164078649	13.4164078649	13.4164078649	13.4164078649
$t = 4$	13.4164078649	13.4164078649	13.4164078649	13.4164078649
$t = 6$	13.4164078649	13.4164078649	13.4164078649	13.4164078649
$t = 8$	13.4164078649	13.4164078649	13.4164078649	13.4164078649
$t = 10$	13.4164078648	13.4164078648	13.4164078648	13.4164078648

Table 5. Discrete mass Q_2 under different mesh steps h and τ_F at various times.

Present Scheme				
	$\left(\frac{1}{2}, \frac{1}{4}\right)$	$\left(\frac{1}{4}, \frac{1}{16}\right)$	$\left(\frac{1}{8}, \frac{1}{64}\right)$	$\left(\frac{1}{16}, \frac{1}{256}\right)$
$t = 0$	8.9442719099	8.9442719099	8.9442719099	8.9442719099
$t = 2$	8.9442719099	8.9442719099	8.9442719099	8.9442719099
$t = 4$	8.9442719099	8.9442719099	8.9442719099	8.9442719099
$t = 6$	8.9442719099	8.9442719099	8.9442719099	8.9442719099
$t = 8$	8.9442719099	8.9442719099	8.9442719099	8.9442719099
$t = 10$	8.9442719099	8.9442719099	8.9442719099	8.9442719099

Table 6. Discrete energy E under different mesh steps h and τ_F at various times.

Present Scheme				
	$\left(\frac{1}{2}, \frac{1}{4}\right)$	$\left(\frac{1}{4}, \frac{1}{16}\right)$	$\left(\frac{1}{8}, \frac{1}{64}\right)$	$\left(\frac{1}{16}, \frac{1}{256}\right)$
$t = 0$	34.7628720201	34.7781529556	34.7819964190	34.7829587447
$t = 2$	34.7647712611	34.7781634038	34.7819965109	34.7829587460
$t = 4$	34.7537001446	34.7780876049	34.7819962655	34.7829587461
$t = 6$	34.7185711285	34.7778355542	34.7819952701	34.7829587428
$t = 8$	34.6591320134	34.7773916731	34.7819934746	34.7829587360
$t = 10$	34.5775373861	34.7767645581	34.7819909256	34.7829587262

Finally, we present the long-time behavior of the $u(x,t)$ and $\rho(x,t)$ using the proposed scheme with the parameter $x_L = -40, x_R = 160, T = 80, h = 1/8, \tau_F = 1/64$. The waveforms of $u(x,t)$ and $\rho(x,t)$ at $t = 0, 40$, and 80 obtained from the present scheme are illustrated in Figure 7. From the figure, it is evident that the waveforms at three different time instances are nearly identical. This observation strongly indicates the high accuracy of our proposed scheme. The long-time errors in $u(x,t)$ and $\rho(x,t)$ over the time interval $[0, 80]$ are presented in Figure 8. Although the errors of the proposed scheme increase over time, the rate of growth is relatively slow, which also indicates the high effectiveness of the proposed scheme.

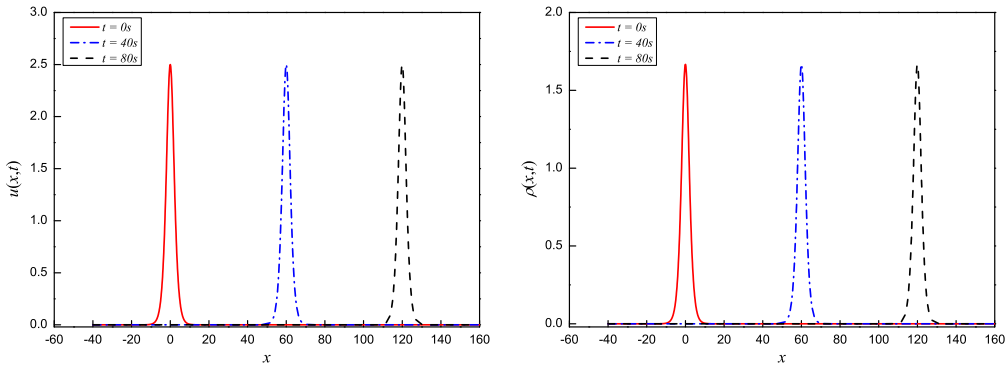

(**a**) (**b**)

Figure 7. Long−time behavior of $u(x,t)$ (**a**) and $\rho(x,t)$ (**b**) under mesh steps with $h = 1/8, \tau_F = 1/64$.

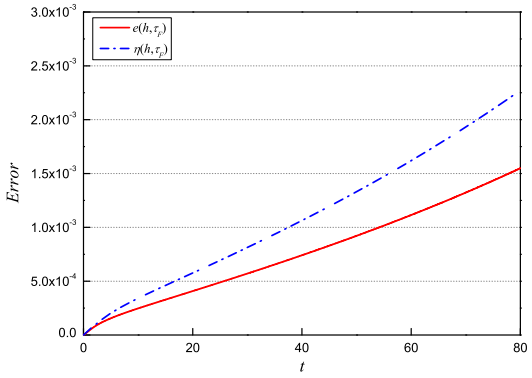

Figure 8. Errors in long-time behavior of $u(x,t)$ and $\rho(x,t)$ with $h = 1/8, \tau_F = 1/64$.

6. Conclusions

In this paper, based on a two-level time-mesh technique, a novel finite difference scheme with a second-order convergence rate in time and a fourth-order convergence rate in space is developed for effectively solving the SRLW Equation (Equation (1)). The proposed scheme is nonlinear on the coarse time-mesh and linear on the fine time-mesh to make it easier to implement. The proposed scheme offers several advantages over existing methods, including improved efficiency and accuracy. We performed a convergence and stability analysis of the proposed scheme; compared to the nonlinear scheme in [16], the proposed scheme not only maintains the same errors and convergence rates as the nonlinear scheme but can also save in computational time, which makes the proposed scheme a valuable tool for practical applications. Moreover, a comparison of the errors obtained using the previous TT-M difference scheme in [27] and the proposed scheme is presented. The results indicate that our proposed scheme exhibits significantly smaller errors than the previous TT-M scheme. The higher accuracy of our scheme ensures stable and reliable solutions throughout the simulation. We also plotted the errors against the CPU time for three methods and found that our proposed scheme is the cheapest of the three schemes in the comparison in terms of CPU time. Finally, the discrete conservation laws were investigated and the long-time simulations that demonstrate the waveform's preservation were conducted to illustrate the effectiveness of the proposed scheme. Overall, the proposed numerical scheme for the SRLW equation is more accurate and efficient than other earlier schemes in the literature. The new difference scheme presents an important advancement in numerical methods for solving the SRLW equation. However, as shown in Figure 8, one of the shortcomings of our scheme is that the error will become large over a very long simulation time. This will be addressed and enhanced through the use of alternative methods in our future work.

Author Contributions: Conceptualization, J.G.; methodology, J.G.; software, J.G. and S.H.; validation, S.H., Q.B., and E.B.; formal analysis, J.G. and S.H.; writing—original draft preparation, J.G.; writing—review and editing, J.G. and S.H.; funding acquisition, S.H., Q.B., and E.B. All authors have read and agreed to the published version of the manuscript.

Funding: Basic Scientific Research Funds of Subordinate Universities of Inner Mongolia (No. ZSLJ202213).

Data Availability Statement: All data were computed using our method.

Acknowledgments: We are grateful to the anonymous reviewers for their valuable suggestions and comments.

Conflicts of Interest: The authors declare that the research was conducted in the absence of any commercial or financial relationships that could be construed as a potential conflict of interest.

References

1. Seyler, C.E.; Fenstermacher, D.L. A symmetric regularized-long-wave equation. *Phys. Fluids* **1984**, *27*, 4–7. [CrossRef]
2. Xu, F. Application of Exp-function method to symmetric regularized long wave (SRLW) equation. *Phys. Lett. A* **2008**, *372*, 252–257. [CrossRef]
3. Abazari, R. Application of (G'/G)-expansion method to travelling wave solutions of three nonlinear evolution equation. *Comput. Fluids* **2010**, *39*, 1957–1963. [CrossRef]
4. Hussain, A.; Jhangeer, A.; Abbas, N.; Khan, I.; Nisar, K.S. Solitary wave patterns and conservation laws of fourth-order nonlinear symmetric regularized long-wave equation arising in plasma. *Ain Shams Eng. J.* **2021**, *12*, 3919–3930. [CrossRef]
5. Manafian, J.; Zamanpour, I. Exact travelling wave solutions of the symmetric regularized long wave (SRLW) using analytical methods. *Stat. Optim. Inf. Comput.* **2014**, *2014*, 47–55.
6. Bekir, A. New solitons and periodic wave solutions for some nonlinear physical models by using the sine–cosine method. *Phys. Scr.* **2008**, *77*, 045008. [CrossRef]
7. Guo, B. The spectral method for symmetric regularized wave equations. *J. Comput. Math.* **1987**, *5*, 297–306.
8. Zheng, J.; Zhang, R.; Guo, B. The Fourier pseudo-spectral method for the SRLW equation. *Appl. Math. Mech.* **1989**, *10*, 801–810.
9. Shang, Y.; Guo, B. Analysis of chebyshev pseudospectral method for multi-dimentional generalized SRLW equations. *Appl. Math. Mech.* **2003**, *24*, 1035–1048.
10. Fang, S.; Guo, B.; Qiu, H. The existence of global attractors for a system of multi-dimensional symmetric regularized wave equations. *Commun. Nonlinear Sci. Numer. Simul.* **2009**, *14*, 61–68.
11. Wang, T.C.; Zhang, L.M.; Chen, F.Q. Conservative schemes for the symmetric regularized long wave equations. *Appl. Math. Comput.* **2007**, *190*, 1063–1080. [CrossRef]
12. Bai, Y.; Zhang L.M. A conservative finite difference scheme for symmetric regularized long wave equations. *Acta Math. Appl. Sin.* **2007**, *30*, 248–255.
13. Xu, Y.C.; Hu, B.; Xie, X.P.; Hu, J.S. Mixed finite element analysis for dissipative SRLW equations with damping term. *Phys. Fluids* **2012**, *218*, 4788–4797. [CrossRef]
14. Yimnet, S.; Wongsaijai, B.; Rojsiraphisal, T.; Poochinapan, K. Numerical implementation for solving the symmetric regularized long wave equation. *Appl. Math. Comput.* **2016**, *273*, 809–825. [CrossRef]
15. Nie, T. A decoupled and conservative difference scheme with fourth-order accuracy for the symmetric regularized long wave equations. *Appl. Math. Comput.* **2013**, *219*, 9461–9468. [CrossRef]
16. Hu, J.; Zheng, K.; Zheng, M. Numerical simulation and convergence analysis of a high-order conservative difference scheme for SRLW equation. *Appl. Math. Model.* **2014**, *38*, 5573–5581. [CrossRef]
17. Kerdboon, J.; Yimnet, S.; Wongsaijai, B.; Mouktonglang, T.; Poochinapan, K. Convergence analysis of the higher-order global mass-preserving numerical method for the symmetric regularized longwave equation. *Int. J. Comput. Math.* **2021**, *98*, 27. [CrossRef]
18. He, Y.Y.; Wang, X.F.; Cheng, H.; Deng, Y.Q. Numerical analysis of a high-order accurate compact finite difference scheme for the SRLW equation. *Appl. Math. Comput.* **2022**, *418*, 126837. [CrossRef]
19. Li, S.G. Numerical study of a conservative weighted compact difference scheme for the symmetric regularized long wave equations. *Numer. Methods Partial. Differ. Equ.* **2018**, *35*, 60–83. [CrossRef]
20. He, Y.Y.; Wang, X.F.; Zhong, R.H. New linearized fourth-order conservative compact difference scheme for the SRLW equations. *Adv. Comput. Math.* **2022**, *48*, 27. [CrossRef]
21. Liu, Y.; Yu, Z.D.; Li, H.; Liu, F.W.; Wang, J.F. Time two-mesh algorithm combined with finite element method for time fractional water wave model. *Int. J. Heat Mass Transf.* **2018**, *120*, 1132–1145. [CrossRef]
22. Yin, B.L.; Liu, Y.; Li, H.; He, S. Fast algorithm based on TT-M FE system for space fractional Allen-Cahn equations with smooth and non-smooth solutions. *J. Comput. Phys.* **2019**, *379*, 351–372. [CrossRef]
23. Qiu, W.L.; Xu, D.; Guo, J.; Zhou, J. A time two-grid algorithm based on finite difference method for the two-dimensional nonlinear time-fractional mobile/immobile transport model. *Numer. Algorithms* **2020**, *85*, 39–58. [CrossRef]
24. Xu, D.; Guo, J.; Qiu, W.L. Time two-grid algorithm based on finite difference method for two-dimensional nonlinear fractional evolution equations. *Appl. Numer. Math.* **2019**, *152*, 169–184. [CrossRef]
25. Niu, Y.X.; Liu, Y.; Li, H.; Liu, F.W. Fast high-order compact difference scheme for the nonlinear distributed-order fractional Sobolev model appearing in porous media. *Math. Comput. Simul.* **2023**, *203*, 387–407. [CrossRef]
26. He, S.; Liu, Y.; Li, H. A time two-mesh compact difference method for the one-dimensional nonlinear schrödinger equation. *Entropy* **2022**, *24*, 806. [CrossRef] [PubMed]
27. Gao, J.Y.; He, S.; Bai, Q.M.; Liu, J. A Time Two-Mesh Finite Difference Numerical Scheme for the Symmetric Regularized Long Wave Equation. *Fractal Fract.* **2023**, *7*, 487. [CrossRef]
28. Zhou, Y.L. *Application of Discrete Functional Analysis to the Finite Difference Method*; International Academic Publishers: Beijing, China, 1990.